

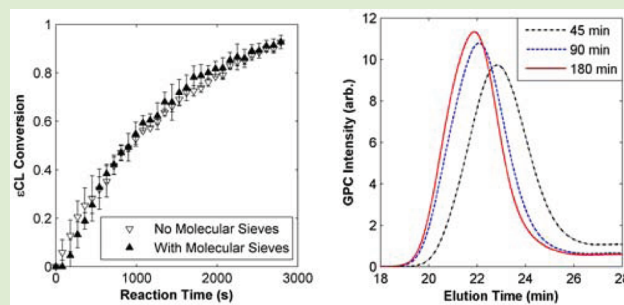
## Increasing Molecular Mass in Enzymatic Lactone Polymerizations

Santanu Kundu,<sup>†,‡</sup> Peter M. Johnson,<sup>†,§</sup> and Kathryn L. Beers\*<sup>‡</sup>

Polymers Division, National Institute of Standards and Technology, Gaithersburg, Maryland 20899, United States

## Supporting Information

**ABSTRACT:** Using a model developed for the enzyme-catalyzed polymerization and degradation of poly( $\epsilon$ -caprolactone), we illustrate a method and the kinetic mechanisms necessary to improve molecular mass by manipulating equilibrium reactions in the kinetic pathway. For these polymerization/degradation reactions, a water/linear chain equilibrium controls the number of chains in solution. Here, we control the equilibrium by adding water-trapping molecular sieves in the batch polymerization reactions of  $\epsilon$ -caprolactone. While ring-opening rates were mostly unaffected, the molecular mass shifted to higher molecular masses after complete conversion was reached, and a good agreement between the experimental and modeling results was found. These results provide a framework to improve the molecular mass for enzyme-catalyzed ring-opening polymerization of lactone.



Industrial production of polymers often requires precise control of molecular mass and molecular mass distribution. A detailed knowledge of the underlying polymerization mechanisms is generally required to generate a consistent and predictable range of polymer properties. At the moment, such control is difficult to achieve in polymerization routes using enzymes as catalysts because the reaction pathways are very complex and not fully understood. In the case of lipase-catalyzed polymerization of  $\epsilon$ -caprolactone ( $\epsilon$ CL), the application of enzymes resulted in milder processing conditions, but the molecular mass of the products is often low and has a high polydispersity index.<sup>1–5</sup> Determining methods to improve these end products could lead to wider scale applications of enzymes in industrial settings, thus, providing an alternative sustainable manufacturing route to metal catalysts.<sup>1,2</sup> Through a combination of experimental studies, the dominant kinetic reactions in enzymatic polymerization have been determined.<sup>3–5</sup> Key reaction conditions include the initial water concentration, enzyme stability, and active-site availability.<sup>3–7</sup> In particular, the presence of water is important to achieve higher monomer conversion, as water acts as an initiator, which drives the polymerization reactions forward.<sup>3–6</sup> At the same time, a high initial water concentration reduces the final molecular mass significantly by increasing the number of polymer chains present in the system.<sup>3–6</sup>

Because enzymatic polymerization consists of multiple simultaneous kinetic reactions, experimental results are limited in predicting new polymerization conditions. Previously published work detailed a kinetic model for lactone polymerization based on experiments designed to confirm kinetic mechanisms. The model predicts monomer conversion, molecular mass and molecular mass distribution of polymers, both cyclic and linear, and incorporated the dominant kinetic

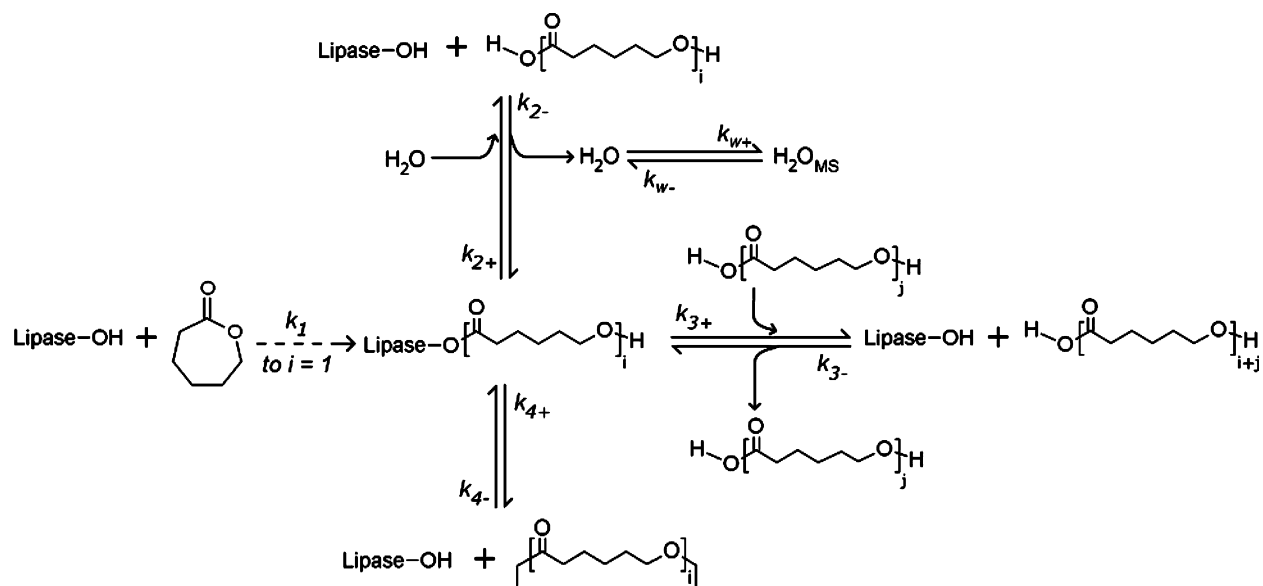
reactions into a single kinetic pathway.<sup>4</sup> Similar to other kinetic models successfully developed for various polymerization reactions,<sup>8–10</sup> this model predicted the molecular mass distribution and ring-opening rate as a function of reaction time and the amount of water present in the system. This model tracks all polymer/oligomer chains unlike previous approaches using a reactive group model or method of moments,<sup>11</sup> which cannot predict the overall molecular mass distribution correctly.

Both modeling and experimental studies demonstrate a need to control water concentration to synthesize high molecular mass chains, but limited control methods are available in a batch reaction. As shown in the previous publications, a high initial water concentration increases the rate of the ring-opening step by increasing the availability of enzyme active sites through initiation reactions.<sup>4,5</sup> However, higher water concentration causes an increased number of polymer chains and the corresponding decrease of final molar mass. If water can be removed from the system once all the  $\epsilon$ CL rings are open, higher molecular mass polymers can be obtained. Therefore, an ideal water concentration profile would have the water concentration present in the system decrease significantly during the course of the reaction. Here, we have extended the previously developed kinetic model to include molecular sieves as a water trapping agent and to predict the corresponding change of reaction rates and the molecular mass of polymer products. Adding molecular sieves was predicted to remove the water from the system slowly,<sup>12</sup> only after the ring-opening step completed, resulting in a high reaction rate and higher

Received: November 30, 2011

Accepted: February 2, 2012

Published: February 10, 2012

Scheme 1. Modeled Kinetic Reactions in Enzyme-Catalyzed Poly( $\epsilon$ -caprolactone) Synthesis in the Presence of Molecular Sieves (MS)<sup>a</sup>

<sup>a</sup>Subscripts on kinetic rate parameters denote the reaction step number.

molecular mass end products. Results of the kinetic model have been validated with experimental data, which show an increase in higher molecular mass PCL chains. Good agreement between experimental and modeling results supports the strong predictive capability of the model, which can be further used to test other reaction conditions.

Experimental studies of lipase catalyzed enzymatic polymerization reactions have been performed in batch reactors.<sup>4,5</sup> In typical batch reactions, polymerization of  $\epsilon$ CL is performed using 2 mL toluene, 1 mL  $\epsilon$ CL, and 100 mg of Novozym N435 beads. (Immobilized *Candida antarctica* Lipase B enzymes on porous polymers beads. Equipment, instruments, or materials are identified in the paper to adequately specify the experimental details. Such identification does not imply recommendation by National Institute of Standards and Technology, nor does it imply the materials are necessarily the best available for the purpose). The reactions were performed at 70 °C. For the polymerization reactions with molecular sieves, 100 mg of molecular sieves were also added to the reaction flask at the start of the reaction. As described in an earlier publication, Raman spectroscopy was used to quantify conversion as a function of time by monitoring the  $\epsilon$ CL ring stretching peak.<sup>4,5,13</sup>

Scheme 1 displays the kinetic pathways involved in the immobilized lipase catalyzed polymerization reaction of  $\epsilon$ CL. Detailed analysis of the model and mechanisms that create the final PCL distribution were covered in depth elsewhere.<sup>4</sup> Briefly, the model included enzymatic ring-opening of  $\epsilon$ CL and three different reaction equilibria from enzyme activated PCL chains. The first equilibria included enzyme activated PCL chains reacting with water at the enzyme-PCL ester, creating a linear PCL chain. The reverse equilibrium step generates water when the ester reforms from the carboxylic acid end group. This equilibrium controlled the number of chains present in the solution at any given time. The second equilibrium was the polycondensation of an enzyme-activated chain with a free linear PCL chain, with the reverse step being an enzymatic scission of a PCL chain into an enzyme-activated chain and a

smaller free linear PCL chain. The final equilibria consisted of ring closing of enzyme-activated chains to form cyclic chains, which could be reversed if the enzyme cleaves an ester in a cyclic PCL chain.

Because the water equilibrium step effectively controls the number of free chains in solution, the molecular mass distribution of PCL chains is strongly correlated with the initial water concentration. Previous studies have shown the addition of water will reduce the molecular mass in enzymatic PCL polymerization; therefore, to increase the molecular mass, the absolute water concentration must be reduced.<sup>5,6</sup> However, the decrease of initial water concentration significantly would reduce the monomer conversion, as water is involved in the initiation step.<sup>5,6</sup> An alternative would be to maintain high initial water concentration, then remove water from the system to increase the molar mass of the products.

To incorporate this possibility into the model, an additional step describing the removal of water using molecular sieves was considered. The equilibrium adsorption step is shown in eq 1.



where MS is the molecular sieves pore sites,  $\text{H}_2\text{O}_{\text{MS}}$  is water trapped within the molecular sieve, and  $K_w$  is the equilibrium adsorption constant.  $K_w = k_{w+}/k_{w-}$ , where  $k_{w+}$ , and  $k_{w-}$  are adsorption rate parameters for the forward and backward steps of the equilibrium. If only this equilibrium step is considered and the water concentration is much smaller than the number of molecular sieve trapping sites, the kinetic rates simplify to

$$\begin{aligned} \frac{d[\text{H}_2\text{O}]}{dt} &= -\frac{d[\text{H}_2\text{O}_{\text{MS}}]}{dt} \\ &= -k_{w+}[\text{H}_2\text{O}] + k_{w-}[\text{H}_2\text{O}_{\text{MS}}] \end{aligned} \quad (2)$$

To obtain an estimate of these adsorption parameters, Karl Fischer titration measurements were performed on toluene solutions, which were continuously stirred with both molecular

sieves (0.5 nm) and N435 beads, the primary source of water in the system. As shown in Figure 1, the water concentration

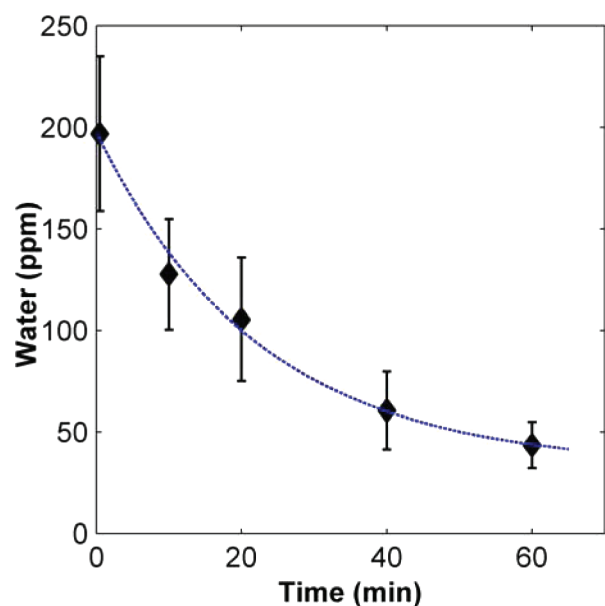


**Figure 1.** Water concentration as a function of time for toluene solutions with N435 beads and molecular sieves (0.5 nm). Equation 2 is fitted to the experimental results (dashed line).

decreased with time. Note that the rate at which water was removed from the system was quite slow, with  $t_{1/2} \approx 1600$  s. Equation 2 was fitted to the experimental data with  $k_{w+} = 8.1 \times 10^{-4} \text{ s}^{-1}$  and  $k_{w-} = 1.5 \times 10^{-4} \text{ s}^{-1}$  as best fit. Error results for these parameters are given in the Supporting Information.

This adsorption step was included in the current kinetic model, requiring one additional species to be tracked. The initial concentrations and kinetic rate parameters remained unchanged from the previous work and are reported in the Supporting Information. The kinetic model was run for systems containing up to 3000 repeat unit chains, and equivalent  $\epsilon$ CL and water initial conditions were used for reactions with and without molecular sieves. The model results provided concentrations for  $\epsilon$ CL, water, enzyme bound chains, linear PCL chains, and cyclic PCL chains. Kinetics models were calculated for a reaction time of 18000 s. During polymerization reactions the initial water present in the system can remain in solution (toluene), be trapped in molecular sieves, or be incorporated into linear PCL chains. Here, our model tracks these species containing the initial water concentration as a function of reaction time (Figure S3).

Figure 2 shows  $\epsilon$ CL conversion and number average molecular mass as a function of time for modeled reactions with and without molecular sieves. In both cases, the model predicts an equivalent  $\epsilon$ CL conversion. This result was not unexpected because the water concentration is reduced to nearly zero due to the ring-opening step (Figure S3, Supporting Information). Similarly,  $M_n$  is also equivalent throughout  $\epsilon$ CL conversion. As the water adsorption rate is much slower compared to the ring-opening step, molecular sieves fail to remove water during  $\epsilon$ CL ring-opening polymerization. However, after polymerization was complete, the water concentration equilibrated to a nonzero level. This shift caused an effective increase in the molecular mass even in the control case after  $\epsilon$ CL conversion was completed, but plateaus once

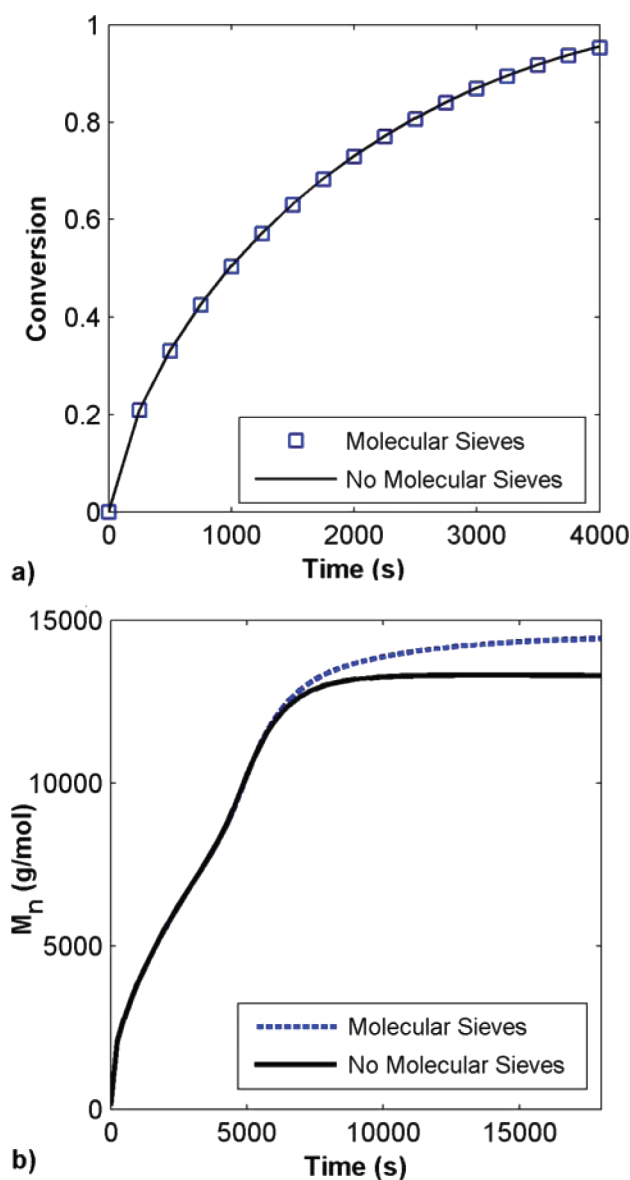


**Figure 2.** Model prediction of  $\epsilon$ CL conversion (a) and number average molecular mass (b) calculated from modeled polymerization reactions with and without molecular sieves.

equilibrium is reached. In the molecular sieve model, detectable fractions of the absolute water concentration begin decreasing in the system once  $\epsilon$ CL conversion was completed. This reduction in water caused an imbalance in the water/linear chain equilibrium, and the enzymatic pathway maintained equilibrium by reducing the number of free linear PCL chains. Using the current model parameters, number average molecular mass ( $M_n$ ) for the molecular sieve model is 15% higher than the control system. This increase was a result of 15% of the total water being trapped within the molecular sieves. Molecular mass as a function of time is shown in the Supporting Information (Figure S2b).

With the model predicting an equivalent  $\epsilon$ CL ring-opening kinetics and an increase of molecular mass with the removal of water, experiments were performed to test the efficacy of molecular sieves in  $\epsilon$ CL enzymatic polymerization. Figure 3 shows the conversion as a function of time for reactions with and without molecular sieves. The addition of molecular sieves

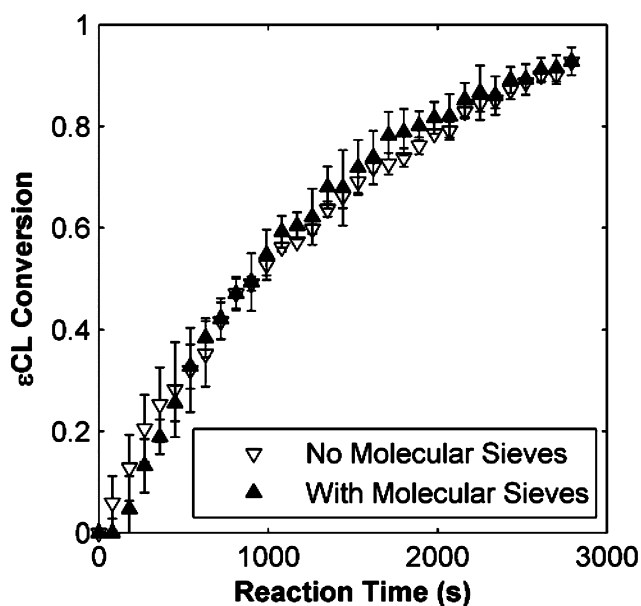


**Figure 3.**  $\epsilon$ CL conversion as measured by in situ Raman spectroscopy for reactions with and without molecular sieves. All measurements were repeated at least three times and the error bars represent one standard deviation.

did not change the Raman spectra in any significant manner. For both systems, the conversion proceeds to over 95% conversion in approximately 2700 s (45 min). At this high conversion, the intensity of the tracked  $\epsilon$ CL peak is insignificant and was difficult to detect using Raman spectroscopy. The reactions were continued until 180 min to investigate the effect of slow water adsorption by molecular sieves. Aliquots were taken at 45, 90, and 180 min for GPC analysis, with the first aliquot corresponding to near complete conversion of  $\epsilon$ CL. GPC results are shown in Figure 4a for a reaction without molecular sieves and Figure 4b for a reaction with molecular sieves. In reactions with molecular sieves, a significant increase in molecular mass over time was observed. In reactions with and without molecular sieves, all samples at 45 min had an equivalent  $M_n$  of  $7800 \pm 1400$  g/mol. For reactions with molecular sieves,  $M_n$  at  $t = 180$  min increased by  $52 \pm 18\%$  as compared to  $M_n$  estimated at  $t = 45$  min. In reactions without molecular sieves, this value increased by 10%, far less than in the molecular sieve reactions.

In comparison to the model, the experimental results confirm the initial  $\epsilon$ CL conversion is unaffected by the molecular sieves. Also as predicted by the model, an increase of molecular mass was observed experimentally, including the slight increase in molecular mass in the control experiment. However, the model underestimates the absolute change in  $M_n$  and the difference in the absolute magnitude of these changes is due to lack of optimized kinetic parameters and assumptions in the kinetic model. For the case without molecular sieves, we used the kinetic parameters that have been estimated from experimental data of  $\epsilon$ CL conversion and molecular mass distributions.<sup>4</sup> For reactions with molecular sieves, a water adsorption step was added to the model and the adsorption equilibrium constant was measured experimentally. As the kinetic pathway involved multiple steps, which are coupled, it is impossible to determine/optimize the kinetic rate constants for all these coupled steps. Improved accuracy in these kinetic parameters would better predict the equilibrium water concentration when

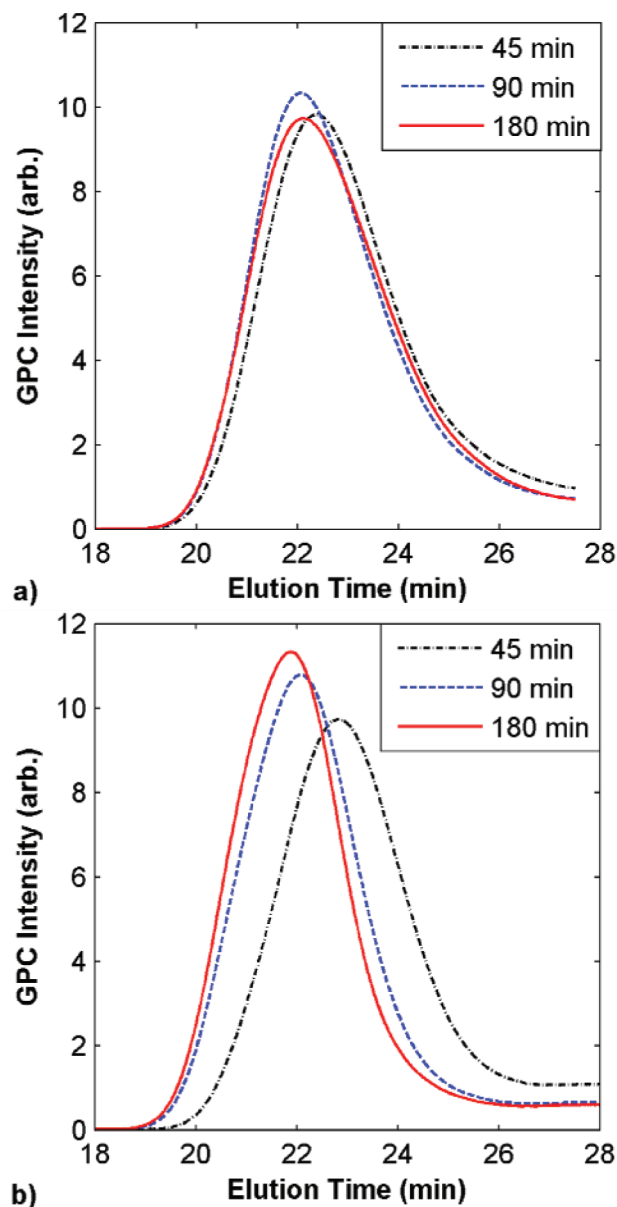


**Figure 4.** GPC traces of PCL distribution for 45, 90, and 180 min for reactions with no molecular sieves (a) and with molecular sieves (b).

$\epsilon$ CL conversion is complete and improve predictive capabilities. Even with current limitations, model results were able to predict the main effects of removal of water using molecular sieves during enzymatic polymerization. To investigate if the removal of trace water was applicable in all enzymatic processes, a degradation study was also performed. A slight increase of molar mass was observed, although the rate of water removal by molecular sieves was not rapid enough to shift the equilibrium reaction toward higher molar mass instead of generation of new polymer chains due to degradation reactions (Supporting Information).

In this work we have modified a recently developed model to incorporate an additional equilibrium step in which water was removed from the reacting system using molecular sieves. Water adsorption by molecular sieves is much slower than the ring-opening step. As a result, the ring-opening kinetics remained unchanged with the addition of molecular sieves. In the later reaction stages, molecular sieves adsorbed water from

the reacting system, causing the equilibrium to shift to higher molecular mass PCL chains. Good agreement between the experimental and modeling results were found, both having similar effects on molecular mass distribution. These results provide a simple framework to improve the molecular mass range for ring-opening polymerization of lactone, and model predictions could be extended to test other mechanisms for enhancing kinetic control. Future research will involve introducing a water trapping reaction that consumes water from the system in a fast and nonequilibrium manner to shift the reaction to even larger molecular mass chains.

## ■ EXPERIMENTAL SECTION

Toluene and  $\epsilon$ CL (Sigma-Aldrich) were dried over 0.5 nm molecular sieves and anhydrous calcium hydride. For PCL degradation experiments, toluene saturated with water was used. To obtain water saturated toluene, a solution of toluene was sonicated with a droplet of water and left for 24 h before separating the immiscible fraction. Novozym N435, *Candida antarctica* lipase B enzymes immobilized on porous  $\sim 400$   $\mu\text{m}$  beads of poly(methyl methacrylate), was obtained from Novozymes (Bagsvaerd, Denmark). Both polymerization and degradation reactions were performed in a 5 mL round-bottom flask at a temperature of 70 °C with constant stirring at 60 rad/s.

A coulometric Karl Fischer water content measurement system (Mettler-Toledo C20, Columbus, OH) was used to measure the water content of toluene solutions. To measure the water adsorption kinetics, 50 mg of N435 beads were introduced in 1.5 mL of toluene solution and gently stirred. Water concentration as a function of time was measured from filtered aliquots.

GPC was used to obtain the molecular mass and molecular mass distribution. A Waters system consisting of three mixed bed columns (HR0.5, HR3, and HR4E) was run under following conditions: THF eluent flow rate of 0.35 mL/min, temperature at 30 °C, sample injection volume of 40  $\mu\text{L}$ , and the sample concentration of 5 mg/mL. To calibrate the GPC system a set of five narrow polydispersity polystyrene standards were used. The uncertainty in the measurement of molecular mass is 10%. Mark–Houwink theory was used to convert the polystyrene equivalent molecular masses to PCL molecular masses using the following parameters:  $K_{\text{PS}} = 29.0 \times 10^{-5}$  dL/g,  $K_{\text{PCL}} = 30.6 \times 10^{-5}$  dL/g,  $\alpha_{\text{PS}} = 0.634$ , and  $\alpha_{\text{PCL}} = 0.70$ .<sup>14</sup> Note that Mark–Houwink calculations are less accurate for molecular mass less than 1000 g/mol. Number average relative molecular mass was calculated from GPC traces using only PCL molecular mass above 1000 g/mol.

For polymerization experiments, the ring-opening of  $\epsilon$ CL was monitored using in situ Raman spectroscopy. A Raman Systems (R3000HR) Raman spectrometer equipped with a fiber optic probe with 5 mm focal length and a 785 nm excitation wavelength laser was used. Spectra were collected for 20 s and the wait time between two successive measurements was 110 s. Ring-opening of  $\epsilon$ CL was tracked from the peak area at 696  $\text{cm}^{-1}$  normalized to a toluene peak area at 1002  $\text{cm}^{-1}$ .<sup>4,5,13</sup> All measurements were repeated at least three times and the error bars represent one standard deviation.

## ■ ASSOCIATED CONTENT

### 📄 Supporting Information

Expanded details on rate parameter error for water equilibrium kinetics, kinetic rate parameter modeling with rate constants, modeled GPC traces, linear PCL chain concentration, and water concentration in reactions with and without molecular sieves, molecular mass recovery in degradation reactions. This information is available free of charge via the Internet at <http://pubs.acs.org>.

## ■ AUTHOR INFORMATION

### Corresponding Author

\*E-mail: [beers@nist.gov](mailto:beers@nist.gov).

## Present Addresses

<sup>‡</sup>Dave C. Swalm School of Chemical Engineering, Mississippi State University, Mississippi State, MS 39762.

<sup>§</sup>Department of Materials Science and Engineering, University of Maryland, College Park, MD 20742; Sabic Innovative Plastics, Mt Vernon, IN.

## Author Contributions

<sup>†</sup>These authors contributed equally.

## Notes

The authors declare no competing financial interest.

## ■ REFERENCES

- (1) Kobayashi, S. *Macromol. Rapid Commun.* **2009**, *30*, 237–266.
- (2) Gross, R. A.; Kumar, A.; Kalra, B. *Chem. Rev.* **2001**, *101*, 2097–2124.
- (3) Mei, Y.; Kumar, A.; Gross, R. *Macromolecules* **2003**, *36*, 5530–5536.
- (4) Johnson, P. M.; Kundu, S.; Beers, K. L. *Biomacromolecules* **2011**, *12*, 3337–3343.
- (5) Kundu, S.; Bhangale, A. S.; Wallace, W. E.; Flynn, K. M.; Guttman, C. M.; Gross, R. A.; Beers, K. L. *J. Am. Chem. Soc.* **2011**, *133*, 6006–6011.
- (6) Mei, Y.; Kumar, A.; Gross, R. A. *Macromolecules* **2002**, *35*, 5444–5448.
- (7) Dong, H.; Cao, S.-G.; Li, Z.-Q.; Han, S.-P.; You, D.-L.; Shen, J.-C. *J. Polym. Sci., Part A: Polym. Chem.* **1999**, *37*, 1265–1275.
- (8) Yu, Y.; Storti, G.; Morbidelli, M. *Macromolecules* **2009**, *42*, 8187–8197.
- (9) Achilias, D. S. *Macromol. Theory Simul.* **2007**, *16*, 319–347.
- (10) Johnson, P. M.; Stansbury, J. W.; Bowman, C. N. *Macromolecules* **2007**, *41*, 230–237.
- (11) Sivalingam, G.; Madras, G. *Biomacromolecules* **2004**, *5*, 603–609.
- (12) Joshi, S.; Fair, J. R. *Ind. Eng. Chem. Res.* **1988**, *27*, 2078–2085.
- (13) Hunley, M. T.; Bhangale, A. S.; Kundu, S.; Johnson, P. M.; Waters, M. S.; Gross, R. A.; Beers, K. L. *Polym. Chem.* **2012**, *3*, 314–318.
- (14) Huang, Y.; Xu, Z.; Huang, Y.; Ma, D.; Yang, J.; Mays, J. W. *Int. J. Polym. Anal. Charact.* **2003**, *8*, 383–394.